

Determination of mode-cutoff wavelengths and refractive-index profile of planar optical waveguides with a photon scanning tunneling microscope

E. Bourillot, S. I. Hosain, and J. P. Goudonnet

Laboratoire de Physique, Unité de Recherche Associée Centre National de la Recherche Scientifique 1796, Equipe Optique Submicronique, Université de Bourgogne, Faculté des Sciences Mirande, Boîte Postale 138, 21004 Dijon, France

G. Voirin and G. Kotrotsios

Centre Suisse d'Electronique et de Microtechnique, Recherche et Développement, Rue de la Maladière 71, CH-2007 Neuchâtel, Switzerland

(Received 5 December 1994; revised manuscript received 10 February 1995)

A method, using the photon scanning tunneling microscope, is proposed to measure the mode cutoff wavelengths of a planar optical waveguide with an arbitrary refractive index profile. From the measured values of the cutoff wavelengths, the characteristic thickness and the maximum refractive index of the guiding film are determined. Measurements, performed on a planar waveguide with a complementary error function profile, are in reasonably good agreement with the theoretical calculations.

Planar dielectric waveguides form the basic components of integrated-optic devices. The refractive index profile and the cutoff wavelengths of the various guided modes are the important parameters associated with these guides. A number of methods, to determine the refractive index profile of such waveguides, are available in the literature.¹⁻⁶ In a recent review,⁷ we discussed some of these basic methods citing a substantial number of important articles. On the other hand, the guided mode cutoff wavelengths of planar waveguides can be determined using, for example, the transmission spectrum method.⁸ The optical waveguide characterization still remains a topic of current interest and attempts to develop new techniques to determine the waveguide parameters are still under active consideration⁹ in various laboratories of the world. We feel that one such attempt would be to use a photon scanning tunneling microscope (PSTM) developed since 1989.¹⁰⁻¹² This microscope is based on the principle of frustration of the evanescent field at the air-sample interface when an optical fiber, tapered to a tip by the chemical etching process, is brought very close (a few nanometers) to this interface. Imaging sample surfaces, with a resolution below the Rayleigh diffraction limit ($\sim\lambda/20$ laterally and $\lambda/100$ vertically¹³), has now become a routine work using the PSTM. Now interest lies in other possible applications of this microscope. Among the other applications, the study of the surface plasmons,¹⁴ the accurate determination of the widths of channel optical waveguides,¹⁵ and the study of the evolution of optical power transfer in an integrated optic directional coupler¹⁶ are worth mentioning. Using the PSTM, a method to measure the effective index n_e ($=\beta/k_0$, where β is the propagation constant, $k_0=2\pi/\lambda$ is the wave number in vacuum) of the guided mode of a channel or a planar waveguide has been recently reported.¹⁷ Although the accuracy of this method is less than that using the other standard techniques, no doubt this method demonstrates an interesting application of the PSTM. Motivated by this latter work, we have developed a method, using the PSTM, to measure the cutoff wavelengths of the modes of a graded index planar optical waveguide with an arbitrary refractive index profile.

From these measured values of the cutoff wavelengths, the characteristic thickness and the maximum refractive index of the guiding film (and thus the parameters of the index profile) are then determined using the procedure of Ref. 6.

A detailed account of the construction and the mode of functioning of the PSTM can be found elsewhere.¹⁰⁻¹² The schematic diagram of our experimental setup to measure the mode cutoff wavelengths is shown in Fig. 1. Light from a 500-W xenon lamp is passed through a monochromator, a polarizer, and a focussing lens and is then end-fire coupled into the planar waveguide to excite all the TE modes at a desired exciting wavelength. Although our method can be applied to determine the cutoff wavelengths of TE or TM modes, we have carried out experiments only with the TE modes (which are sufficient to determine the parameters of the refractive index profile). It is well known that the part of the modal field in the air cover above the surface of the waveguide is an evanescent field. An optical fiber tapered to a fine point, which forms the sensing part of the PSTM, is then brought close to the waveguide surface (a few nanometers) with the help of a piezoelectric tube so that it remains within this evanescent field. The fiber tip is shielded from extraneous light coming from the source. Due to the presence of the fiber tip, there is frustration of the evanescent field¹⁰ resulting in tunneling of photons from the waveguide

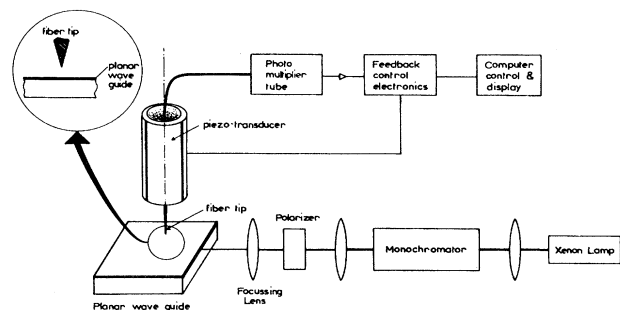


FIG. 1. Block diagram of the experimental setup.

surface to the fiber tip. The light, thus coupled, is guided through the fiber to the photomultiplier and the feedback electronics, and an output signal of intensity I_s is recorded. The presence of this output signal confirms that the fiber tip is within the evanescent field of the guided modes. The fiber tip is no longer displaced from this position because we do not take the image of the waveguide surface. The wavelength of light, λ , is then increased with the help of the monochromator. As λ approaches the cutoff wavelength λ_{cm} of the highest-order excited mode (say, the m th-order mode), the modal field and hence the evanescent field associated with this mode extends more into the air cover. Such a behavior of the modal field, when the cutoff of the mode is approached, is well known.¹⁸ As a result of this, there is an increase in I_s which is registered by the electronic system of the microscope. When λ just exceeds λ_{cm} , this mode disappears causing a fall in I_s as the other existing modes [the highest order being the $(m-1)$ th mode now], which are far from their cutoffs, remain well confined within the waveguide. Hence in our experiment, the fiber tip detects this variation of I_s due to the variation of λ . The position of the cutoff of a mode appears as a peak in the curve showing the variation of output signal with λ . By varying λ in this manner, the cutoff wavelengths of the various modes are obtained in the form of such peaks in the I_s versus λ curve. We would like to mention here that the presence of the fiber tip close to the waveguide surface perturbs very little the propagation characteristics of the various guided modes.^{17,19} This case is similar to that of a prism used as an output coupler to couple light out from the various modes of the waveguide to produce the so-called m lines. The prism is placed with its base very close to the waveguide surface resulting in the coupling of light from the waveguide to the prism by the process of tunneling. This coupling being weak, the perturbation of the basic mode shapes is negligible.²⁰ Following the same arguments, we assume that the perturbation of the guided modes, due to the presence of the fiber tip close to the waveguide surface, is negligible.

For a large number of practical graded index planar optical waveguides, the refractive index profile is written as^{1-3,18}

$$n^2(\xi) = \begin{cases} n_s^2 + (n_f^2 - n_s^2)F(\xi), & \xi \geq 0 \\ n_c^2, & \xi < 0, \end{cases} \quad (1)$$

where n_s and n_c (which are known) are the refractive indexes of the substrate and cover (usually air), respectively, $n_f = n(0)$ is the maximum refractive index at the waveguide-cover interface, $\xi = x/d$ is the normalized coordinate, and d is the characteristic thickness. $F(\xi)$ is the normalized profile function which defines the shape of the profile and satisfies the conditions $F(0) = 1$ and $F(\infty) = 0$. For example, for exponential, Gaussian, and complementary error function profiles, $F(\xi) = e^{-\xi}$, $e^{-\xi^2}$, and $\text{erfc}(\xi)$, respectively.^{18,21} In the present geometry, the x axis is perpendicular to the waveguide surface and the z axis is parallel to the direction of propagation of the modes.

To verify the experimental results on the measurement of λ_{cm} , one needs a rigorous method for calculating this parameter. With this aim, we present here a simple but efficient numerical method for computing the normalized cutoff frequency V_{cm} (and hence λ_{cm}) of the TE_m modes. This parameter is defined as¹⁸

$$V_{cm} = (2\pi/\lambda_{cm})d(n_f^2 - n_s^2)^{1/2}, \quad (2)$$

where λ_{cm} is the corresponding cutoff wavelength. The details of the numerical procedure used to compute the cutoff frequencies of TE_0 and TE_1 modes for a given index profile can be found elsewhere.²¹ However, we present here a brief account of this method for an arbitrary TE_m mode. Using the transformation $G = (dE_y/d\xi)/E_y$, where E_y is the electric-field component associated with the TE_m mode, the wave equation at cutoff of this mode can be written as

$$dG/d\xi = -G^2 - V_{cm}^2 F(\xi), \quad \xi \geq 0. \quad (3)$$

G satisfies the following boundary conditions:²¹

$$G(\xi=0) = V_{cm}\sqrt{\sigma}, \quad G(\xi \rightarrow \infty) = 0, \quad (4)$$

where $\sigma = (n_s^2 - n_c^2)/(n_f^2 - n_s^2)$ is the usual asymmetry parameter. For a given value of σ corresponding to a given profile function $F(\xi)$, the problem of computing V_{cm} then reduces to solving (3) using any standard algorithm so that the boundary conditions (4) are satisfied. For computational purposes, the point $\xi \rightarrow \infty$ is chosen as some finite value of $\xi = \xi_{\max}$ which is much greater than unity. Thus, in the actual computational procedure, $G(\xi_{\max})$ is evaluated instead of $G(\infty)$. ξ_{\max} is varied to improve the accuracy in V_{cm} . However, it may be noted that for the TE_m mode with $m > 0$, there are m values of ξ in the interval $(0, \infty)$ where E_y becomes zero, implying that $G(\xi) = \infty$. Hence, in the neighborhood of these zeros of E_y , one has to switch over to the substitution $H = 1/G = E_y/(dE_y/d\xi)$ which transforms (3) to the following form:

$$dH/d\xi = 1 + V_{cm}^2 H^2 F(\xi), \quad (5)$$

and one continues solving (5) instead of (3) in the neighborhood of the zeros of E_y . Each time $G(\xi) \rightarrow \infty$ [i.e., $H(\xi) = 0$] region is crossed, one switches over to solving Eq. (3) and the process is continued until $G(\xi_{\max})$ is computed: thus in this way one obtains the desired value of V_{cm} .

We present some experimental results on the measurement of cutoff wavelengths to show the effectiveness of our method. The three planar waveguides, denoted A , B , and C , used in our experiment were fabricated at Centre Suisse d'Electronique et de Microtechnique SA, Neuchâtel, Switzerland. The refractive index variation was produced on the glass (BK7) substrate of $n_s = 1.515$ through the exchange of K^+ ions using the ion-exchange process. For each waveguide, $F(\xi) = \text{erfc}(\xi)$ and $n_f = 1.592$ so that $\sigma = 5.414$. The values of d for waveguides A , B , and C are, respectively, 3.354, 4.06, and 6.71 μm . The number of modes, supported by each waveguide at a chosen wavelength, was determined in a separate experiment by exciting the various modes using the prism-coupling technique. Waveguide A supports five TE modes at $\lambda = 633$ nm, the TE_4 mode being the highest-order mode, and waveguides B and C support six and nine modes, respectively. The experimental procedure, as described in the second paragraph, was followed to measure the mode cutoff wavelengths. The wavelength of the incident light was varied from 520 to 750 nm with the help of the monochromator. This range was chosen because the power spectrum of the source has almost a uniform linear variation in this range. The normalized intensity I_s as a function of λ , obtained for waveguides A , B , and C , is presented in Fig. 2. For wave-

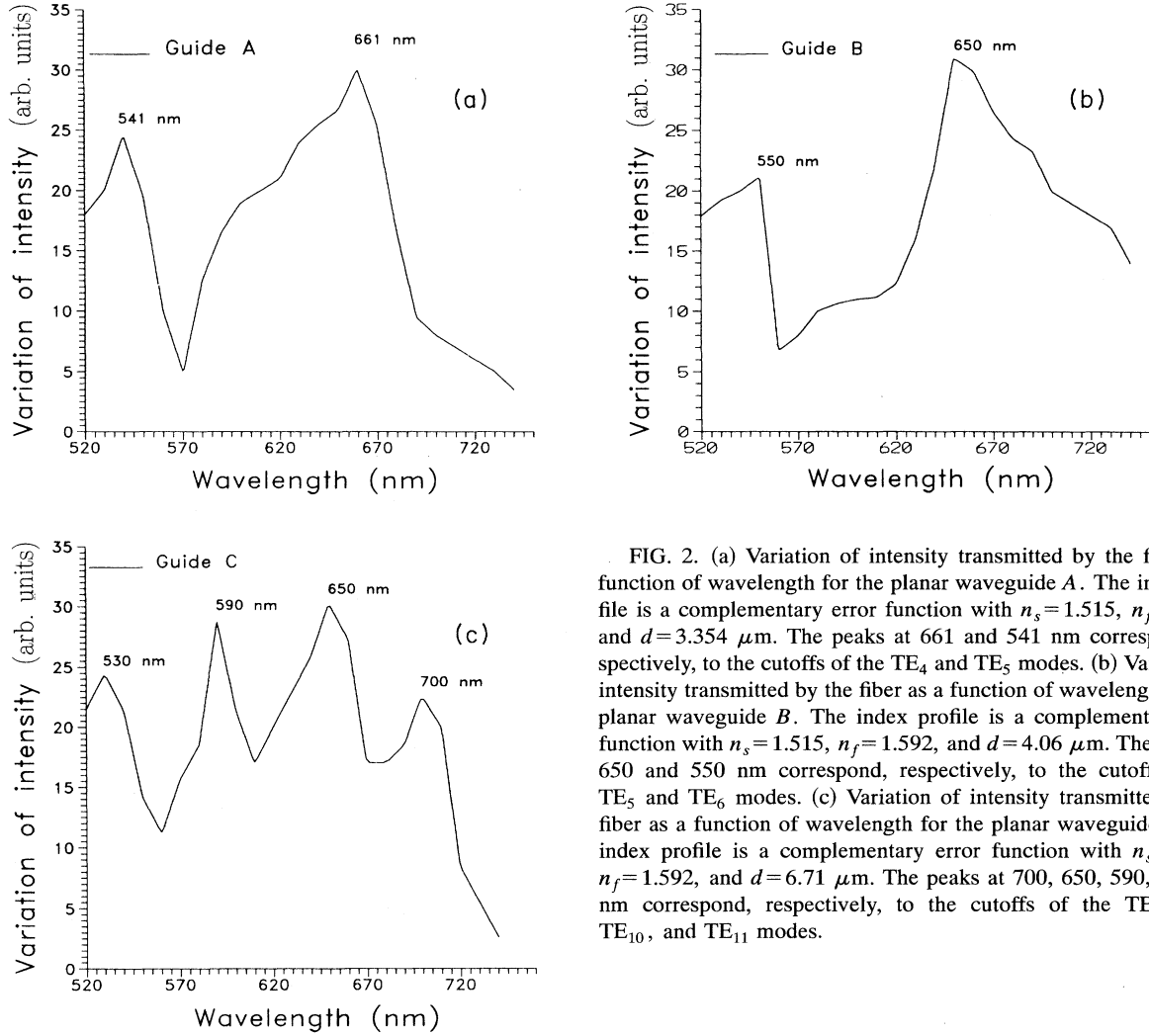


FIG. 2. (a) Variation of intensity transmitted by the fiber as a function of wavelength for the planar waveguide A. The index profile is a complementary error function with $n_s=1.515$, $n_f=1.592$, and $d=3.354 \mu\text{m}$. The peaks at 661 and 541 nm correspond, respectively, to the cutoffs of the TE_4 and TE_5 modes. (b) Variation of intensity transmitted by the fiber as a function of wavelength for the planar waveguide B. The index profile is a complementary error function with $n_s=1.515$, $n_f=1.592$, and $d=4.06 \mu\text{m}$. The peaks at 650 and 550 nm correspond, respectively, to the cutoffs of the TE_5 and TE_6 modes. (c) Variation of intensity transmitted by the fiber as a function of wavelength for the planar waveguide C. The index profile is a complementary error function with $n_s=1.515$, $n_f=1.592$, and $d=6.71 \mu\text{m}$. The peaks at 700, 650, 590, and 530 nm correspond, respectively, to the cutoffs of the TE_8 , TE_9 , TE_{10} , and TE_{11} modes.

guide A, two peaks are observed at 541 and 661 nm. For this waveguide, as the TE_4 mode is the highest-order mode at $\lambda=633 \text{ nm}$, the peak at 661 nm corresponds obviously to the cutoff of the TE_4 mode. Thus, the peak around 541 nm corresponds to the cutoff of the TE_5 mode because the cutoff wavelength of this mode is less than that of the TE_4 mode. The experimental values of the mode cutoff wavelengths of waveguides B and C are obtained in a similar manner from Figs. 2(b) and 2(c). The experimental as well as the calculated values (obtained by using our numerical procedure) of the cutoff wavelengths are summarized in Table I. From the table we observe that, using the PSTM method presented here, the mode cutoff wavelengths are measured with a very good accuracy (with respect to the calculated values) for waveguides supporting less number of modes. We have found that the mode cutoff wavelengths can be measured by this method even for waveguides of the type C supporting up to 12 or 13 modes in which the separation between the mode cutoff wavelengths is of the order of 50 nm. We would like to point out here that the other existing methods⁸ discuss neither the measurement accuracy of the cutoff wavelengths nor the separation between two successive cutoff wavelengths.

Having thus established a PSTM-based method for experimentally measuring the mode cutoff wavelengths, we next determine n_f and d from these measured values of the cutoff wavelengths using a recent method⁶ proposed theoretically. For the convenience of the reader, we briefly describe this method here. As in most of the characterization procedures,¹⁻⁷ this method also assumes a specific form for

TABLE I. Cutoff wavelengths of TE_m modes of the planar waveguides with $F(\xi)=\text{erfc}(\xi)$, $n_s=1.515$, and $n_f=1.592$.

Waveguide	Effective thickness $d (\mu\text{m})$	Mode	Cutoff wavelengths	
			Experimental (μm)	Calculated (μm)
A	3.354	TE_4	0.661 ± 0.001	0.6605
		TE_5	0.541 ± 0.001	0.5419
B	4.060	TE_5	0.650 ± 0.001	0.6560
		TE_6	0.550 ± 0.001	0.5562
C	6.710	TE_8	0.700 ± 0.001	0.7048
		TE_9	0.650 ± 0.001	0.6313
		TE_{10}	0.590 ± 0.001	0.5716
		TE_{11}	0.530 ± 0.001	0.5222

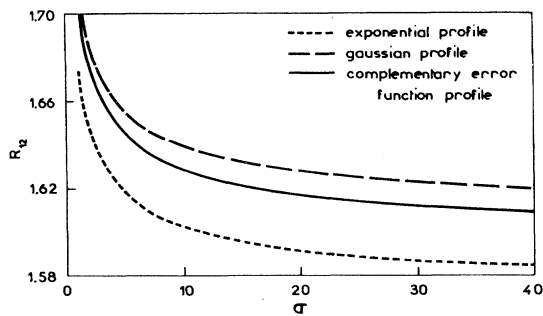


FIG. 3. R_{12} ($=V_{c2}/V_{c1}$) as a function of σ (asymmetry parameter) for three different index profiles of a planar waveguide.

$F(\xi)$ which is judiciously chosen keeping in view the waveguide fabrication process. Neglecting the variation of $(n_f^2 - n_s^2)^{1/2}$ with wavelength, one can write $V_{cm'}/V_{cm} = \lambda_{cm}/\lambda_{cm'}$. V_{cm} depends on σ and $F(\xi)$ and thus, for a given $F(\xi)$, the ratio $R_{mm'} = \lambda_{cm}/\lambda_{cm'}$ is a function of σ alone.⁶ This functional dependence $R_{mm'}(\sigma)$ can easily be determined using our numerical procedure. As an illustration, in Fig. 3 we have plotted $R_{12}(\sigma)$ (corresponding to the TE₁ and TE₂ modes) as a function of σ for an exponential, a Gaussian, and a complementary error function profile. It is important to note that this functional dependence exhibits an asymptotic behavior for values of σ below or above a certain value. Such an asymptotic behavior is intrinsic to all kinds of profiles and to all orders of mode.⁶ The first step of the characterization procedure is then to form the ratio $\lambda_{cm}/\lambda_{cm'}$ of the experimentally measured cutoff wavelengths. Assuming a profile and fitting this measured ratio to the functional dependence $R_{mm'}(\sigma)$ obtained by the numerical method, the value of σ for the waveguide is computed. As n_s and n_c are known, the value of n_f is calculated using the defining equation for σ . The values of V_{cm} for different modes, corresponding to this value of σ , are then numerically computed. Substituting in Eq. (2) the measured values of λ_{cm} 's and the value of n_f already determined, an average value of d is calculated.

To demonstrate the effectiveness of this method, we now assume that the parameters of waveguide A are unknown. We then use the method to determine these parameters using the experimentally measured values of the TE₄ and TE₅ mode cutoff wavelengths presented in Table I. We assume the profile function to be a complementary error function, as such a profile is associated with a waveguide fabricated by the ion-exchange process.²⁰ Following the various steps of the method discussed in the preceding paragraph, we obtain $n_f = (1.605 \pm 0.011)$ and $d = (3.087 \pm 0.195) \mu\text{m}$. These values are in good agreement with the actual values $n_f = 1.592$ and $d = 3.354 \mu\text{m}$ presented in Table I. As discussed in Ref. 6, an important limitation of this method is that σ must not be very large or very small. If σ is too small or too large to lie in the asymptotic regions of the $R_{mm'}$ versus σ curve (see Fig. 3), then a slight deviation in the cutoff wavelength from its actual value introduces an appreciably large error in the computed values of n_f and d . This rise in the error is not due to a bad assumption of $F(\xi)$, but it is intrinsic to all profiles due to the asymptotic behavior of $R_{mm'}$ with σ . The value of σ should be preferably more than 5 and less than 35 for all the profiles. Fortunately, the value of σ lies in this range for most of the practical waveguides and we think that this limitation on σ is not very important.

In conclusion, the PSTM has been shown to be a useful tool in the measurement of mode cutoff wavelengths of graded index planar optical waveguides with excellent accuracy. To our knowledge, it is the first time that the evanescent field associated with the mode is used to determine the mode cutoff wavelengths. The parameters n_f and d of the refractive index profile predicted from these measurements are also in good agreement with their actual values.

This work was supported in part by the BCR Programme CT No. 940027 of the Commission of the European Communities. S.I.H., who is on long-term leave from Physics Department, Ravenshaw College, Cuttack (India), acknowledges the financial support of France Telecom (CNET) and the Région Bourgogne (France).

¹R. Ulrich and R. Torge, *Appl. Opt.* **12**, 2901 (1973).

²P. P. Herrmann, *Appl. Opt.* **19**, 3261 (1980).

³D. Sarid, *Appl. Opt.* **19**, 1606 (1980).

⁴A. C. Boucouvalas, *Electron. Lett.* **19**, 120 (1983).

⁵R. K. Sinha and S. I. Hosain, *J. Opt. Commun.* **10**, 105 (1989).

⁶S. I. Hosain and J. P. Meunier, *IEEE Photonics Technol. Lett.* **3**, 801 (1991).

⁷S. I. Hosain *et al.*, *Fiber Int. Optics* **14**, 89 (1995).

⁸K. Thyagarajan *et al.*, in *Integrated Optics*, edited by N.-P. Nolling and R. Ulrich (Springer Verlag, Heidelberg, 1985); S. I. Najafi and R. V. Ramaswamy (unpublished).

⁹M. Sochacka *et al.*, *Appl. Opt.* **33**, 3342 (1994); R. Tavlykaev *et al.*, *J. Opt. Commun.* **15**, 71 (1994).

¹⁰F. de Fornel *et al.*, *Proc. SPIE* **1139**, 77 (1989).

¹¹R. C. Reddick *et al.*, *Phys. Rev. B* **39**, 767 (1989).

¹²D. Courjon *et al.*, *Opt. Commun.* **71**, 23 (1989).

¹³F. de Fornel *et al.*, *Ultramicroscopy* **42-44**, 422 (1992).

¹⁴P. M. Adam *et al.*, *Phys. Rev. B* **48**, 2680 (1993).

¹⁵E. Bourillot *et al.*, *J. Opt. Soc. Am. A* **12**, 95 (1995).

¹⁶A. G. Choo *et al.*, *Appl. Phys. Lett.* **65**, 947 (1994).

¹⁷Y. Wang *et al.*, *Proc. SPIE* **1793**, 66 (1992).

¹⁸M. J. Adams, *An Introduction to Optical Waveguides* (Wiley, New York, 1981).

¹⁹D. Courjon *et al.*, *Opt. Commun.* **110**, 7 (1994).

²⁰R. G. Hunsperger, *Integrated Optics: Theory and Technology* (Springer Verlag, Berlin, 1985).

²¹A. N. Kaul *et al.*, *IEEE Trans. Microwave Theory Tech.* **34**, 288 (1986).